International Journal of Applied Engineering Research ISSN 0973-4562 Volume 14, Number 13 (2019) pp. 3097-3103
© Research India Publications. http://www.ripublication.com

Artificial Neural Networks (ANN) to Predict Overall Heat Transfer Coefficient and Pressure Drop on a Simulated Heat Exchanger

E. Reynoso-Jardón[1*], A. Tlatelpa-Becerro[2,3], R. Rico-Martínez[4], Calderón-Ramírez M[5] and G. Urquiza[6]

[1] *Manufacturing Engineering Department, Universidad Autónoma de Ciudad Juárez, Juárez, Chihuahua, 32310, México.*

[2] *Robotic Engineering Department, Escuela de Estudios Superiores de Yecapixtla-UAEM, Yecapixtla Morelos, 62820, México.*

[3] *Manufacturing Engineering Department, Universidad Politécnica de Atlautla, Atlautla Edo. México, 56970, México.*

[4] *Chemical Engineering Department, Instituto Tecnológico de Celaya, Celaya Guanajuato, 38010, México.*

[5] *Centros Regionales de Optimización y Desarrollo de Equipo (CRODE), Celaya Guanajuato, 38020, México.*

[6] *Mechanical Engineering Department, Centro de Investigación en Ingeniería y Ciencias Aplicadas (CIICAp)-UAEM, Cuernavaca Morelos, 1001, México.*

Abstract

Computational Fluid Dynamics (CFD) numerical simulations were performed to calculate the maximum overall heat transfer coefficient (U) and minimum pressure drop (Δ_p) for a crossflow heat exchanger using four materials: stainless steel, copper, aluminum and titanium. Transversal and longitudinal sections were modified, obtaining 143 geometries for analysis. With the simulated data, an Artificial Neural Network (ANN) was built to predict the overall heat transfer coefficient and pressure drop as a function of the heat exchanger material. The ANN exhibits maximum deviations, between the predicted and simulated data, below 0.9 y 0.3 % for the pressure drop and air overall heat transfer coefficient respectively. This assisted model reference strategy can be used for material selection in the heat exchanger design considering replacement and cleaning cycles due to corrosion and fouling in other thermal analysis tasks in engineering applications.

Keywords Artificial neural networks, Heat transfer, Heat exchanger, Computational Fluid Dynamics.

INTRODUCTION

Heat exchangers are devices that allow the flow of thermal energy between two or more fluids at different temperatures [1]; they are complex systems due to their geometric configuration that seeks increasing efficiency in the heat transport. Simulations of heat exchangers and other components of thermal systems usually address the steady-state behavior for heat rate prediction required for system design. The temperature gradients depend directly of the geometry of the heat exchanger in relationship to the distribution and position of the elements that transport the fluids. In power generation plants, where heat exchangers are used for the energy generation, the heat exchanger performance depends on several key parameters such as water flow, turbine efficiency and electric generator efficiency, which are related with the cooling capacity during regular operation. Thus, it is important to develop design that allow for the proper selection of the heat exchanger configuration and its material, possibly including operation parameters such as maintenance cycles and replacement time due to fouling.

Heat transfer and fluid behavior in different heat exchanger configurations have been studied for over 40 years [2,3]. More recently assisted by numerical simulations to describe the flow and heat transfer behavior [4-8], including Computational Fluid Dynamics approaches for the analysis [9]. Software packages, such as Fluent, have been applied for 2D and 3D simulations of heat exchangers, achieving a better understanding of the influence of the geometry and materials [10.11]. Improving the efficiency of the heat exchanger design and the development of tools for such a purpose, remain, for the most part, and active research topic [12-19].

In this contribution, Computational Fluid Dynamics (CFD) is applied for the analysis of a crossflow heat exchanger seeking to establish more efficient strategies for finding the optimum design; Data generated from CFD simulations are used to build a surrogate ANN model that includes the material type as part of the variables. Such model may ease the effort in finding the appropriate material taking into account such factors as maintenance and replacement cycles.

ANNs have been used to predict the heat transfer coefficients, performance, pressure drop and dynamic control in thermal systems [20]. ANN also have been used to substitute the dynamical heat exchanger models for complex geometries and predict outlet temperatures, mass flow rates [21], Nusselt numbers and friction factors for finned tubes heat exchangers [22,23].

PHYSICAL MODEL AND GOVERNING EQUATIONS

A schematic of the heat exchanger studied is shown in Figure 1. This is a crossflow heat exchanger with a triangular array of pipes and water-air as working fluid. This configuration is

widely used in hydroelectric plants to reduce the air temperature used to cool the electric generators using a water flow for that purpose. The heat exchanger dimensions are 0.60 x 0.22 x 2 *m*, pipes have internal and external diameters of 0.01*m* and 0.013*m* taken from a real exchanger in use in the Chicoasén Hydroelectric Generation Plant in Southern Mexico.

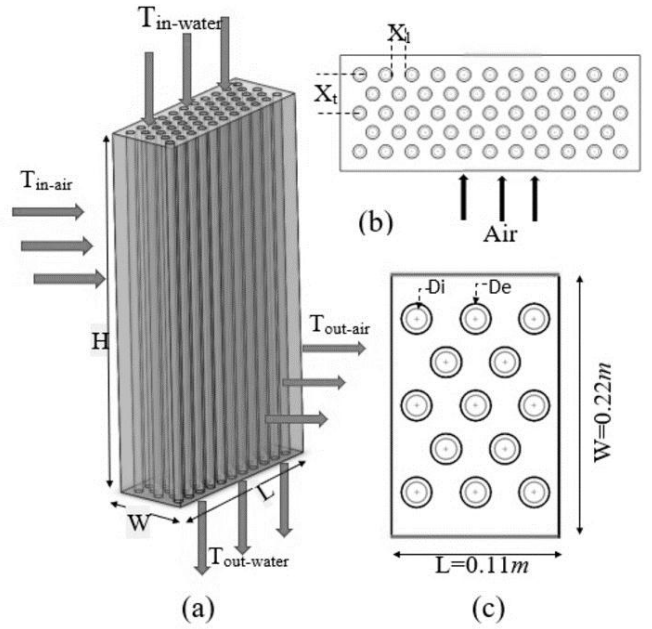

Figure 1. **Figure. 1**. Physical model: a) crossflow heat exchanger: (b) pipe distribution, c) pipe cross section.

A cross section of the heat exchanger is shown in Figure 1c. Following the array of the industrial exchanger six rows and three columns of internal pipes were considered with the following dimensions: *L*=0.22*m* long, *W*=0.11*m* width and *H*=2*m* high, as shown in Figure 1(c). Variations on the internal pipes arrays were studied assisted by the meshes generated by the ICEM software. The transversal and longitudinal sections were varied from 0.064 to 0.054*m* and 0.032 to 0.020*m*. As a result, 143 geometries were modeled considering four materials for the pipes: copper, stainless steel, titanium and aluminum.

Governing equations

The heat exchanger flow usually operates in a turbulent regime [24]. A standard k-ε model was used to analyze the phenomena [25], taking the form of the following governing equations:

Mass conservation equation:

$$\frac{\partial(\rho u_i)}{\partial x_i} = 0 \qquad (1)$$

Momentum conservation equation:

$$\frac{\partial\left(\rho u_i u_j\right)}{\partial x_j} = -\frac{\partial P}{\partial x_i} + \frac{\partial}{\partial x_j}\left(\mu\frac{\partial u_i}{\partial x_j} + \overline{\rho u_i' u_j'}\right) \qquad (2)$$

Energy conservation equation:

$$\frac{\partial(\rho T)}{\partial x_i} + \frac{\partial(\rho u_i T)}{\partial x_i} = \frac{\partial T}{\partial x_i}\left(\frac{k}{Cp}\frac{\partial T}{\partial x_i}\right) \qquad (3)$$

Where: x_i, spatial dimension. u_i, velocity in direction *i.* ρ, fluid density. μ, dinamic viscosity. *P*, pressure and *T,* temperature.

k-ε Model

Turbulent kinetic energy k equation:

$$\frac{\partial}{\partial x_i}(\rho k u_i) = \frac{\partial}{\partial x_j}\left[\left(\mu + \frac{\mu_t}{\sigma_k}\right)\frac{\partial k}{\partial x_j}\right] + G_k + G_b - \rho\varepsilon - Y_M + S_k \qquad (4)$$

Turbulent energy dissipation ε equation:

$$\frac{\partial}{\partial x_i}(\rho\varepsilon u_i) = \frac{\partial}{\partial x_j}\left[\left(\mu + \frac{\mu_t}{\sigma_\varepsilon}\right)\frac{\partial \varepsilon}{\partial x_j}\right] + C_{1\varepsilon}\frac{\varepsilon}{k}\left(G_k + C_{3\varepsilon}G_b\right) - C_{2\varepsilon}\rho\frac{\varepsilon^2}{k} + S_\varepsilon \qquad (5)$$

Here, G_k represents the generation of turbulence kinetic energy due to the mean velocity gradients. G_b is the generation of turbulence kinetic energy due to buoyancy. Y_M represents the contribution of the fluctuating dilatation in compressible turbulence to the overall dissipation rate. μ_t is the turbulent viscosity and is computed by combining k and ε as follows:

$$\mu = \rho C_\mu \frac{k^2}{\varepsilon} \qquad (6)$$

The model constants $C_{1\varepsilon}$, $C_{2\varepsilon}$, C_μ, σ_k and σ_ε have the following default values:

$C_{1\varepsilon} = 1.44,$, $C_{2\varepsilon} = 1.92,$, $C_\mu = .09,$, $\sigma_k = 1.0$ y $\sigma_\varepsilon = 1.3$

Transport Parameters:

The overall heat transfer coefficient, maximum velocity and pressure drop, were calculated by [26]:

$$U = \frac{1}{\frac{1}{h_w}\frac{D_e}{D_i} + \frac{D_e Ln\left(\frac{D_e}{D_i}\right)}{2k} + \frac{1}{h_a}} \qquad (7)$$

Where: convective heat transfer coefficient at both sides is given by:

$$h = \frac{Nu\, k}{D_h} \qquad (8)$$

The Nusselt number was calculated for both water and air flow, respectively by [1]:

$$Nu_w = \frac{\left(\frac{f}{2}\right)\mathrm{Re}_w\ \mathrm{Pr}_w}{1.07 + 12.7\left(\frac{f}{2}\right)^{\frac{1}{2}}\left(\mathrm{Pr}_w^{\frac{2}{3}} - 1\right)} \qquad (9)$$

$$Nu_a = 0.031\, C_n\, \mathrm{Re}_a^{0.8}\, \mathrm{Pr}_a^{0.4} \left(\frac{\mathrm{Pr}_a}{\mathrm{Pr}_w}\right)^{0.25} \left(\frac{X_t}{X_l}\right)^{0.2} \quad (10)$$

Where, *f, Re* and *Pr* are friction factor, Reynolds and Prandtl number, respectively

$$f = \left(1.58\, Ln\, \mathrm{Re}_w - 3.28\right)^{-2} \quad (11)$$

$$\mathrm{Re} = \frac{vD_h\rho}{\mu} \quad (12)$$

$$\mathrm{Pr} = \frac{Cp\mu}{k} \quad (13)$$

The air flow Reynolds number was calculated through two cases. When $2AD > AT$ equation (14) and $2AD < AT$ equation (15). While, water maximum velocity was obtained through numerical simulation.

$$V_{\max} = \frac{X_t}{X_t - D_e} v_a \quad (14)$$

$$V_{\max} = \frac{X_t}{2\left(X_D - D_e\right)} v_a \quad (15)$$

The pressure drop (Δp) is a measure of pipe resistance to the flow, and it is calculated as follows:

$$\Delta p = Nfx \frac{\rho V \max^2}{2} \quad (16)$$

Here, f and x are friction and correction factor, respectively.

COMPUTATIONAL MODEL

Computational Fluid Dynamics (CFD) simulations were developed through the commercial software FLUENT. Heat exchanger was modeled by k-ε turbulence model with turbulent flow heat transfer in 3D. For this case, SIMPLE algorithm [27], interpolation scheme of second degree UPWIND, unstructured type mesh and a convergence study for geometry were used [28].

ARTIFICIAL NEURONAL NETWORKS

The ANNs are defined by their input and output layers, plus a number of hidden layers each comprised of so-called neurons. In theory, an ANN with two hidden layers with the appropriate number of neurons is able to estimate approximately any type of non-linear function. The neurons in each layer are linked to the adjacent layers and the strength of this interconnected configuration is determined by the weights. The interconnected structure leads to a logical relationship between the input and output parameters. The number of neurons for the input and output layers is equal to the input and output variables, respectively. However, in the hidden layer different numbers of neurons can be employed and its number may prevent appropriate optimization of the network. In the network, information is transferred passing through the connections of the neurons in the adjacent layers [29].

Neural networks were applied with a training algorithm to predict the heat transfer global coefficient and pressure drop using the MATLAB toolbox (2010). The ANN consisted of four layers with 5 neurons in the input layer, two hidden layers with 10 neurons each, and 2 neurons in the output layer, as shown in Figure 2. As there is no rigorous way to determine an optimum number of neurons, the choice in the number of neurons in the hidden layers is somewhat arbitrary. Our choice here reflects a compromise between the computational effort required to train the ANN and an estimate of the minimum number of neurons necessary to achieve the objective based on experience. In this process, the choice is tested during the process of validation of the results: in this particular case the optimum number of neurons was determined based on the minimum value of MSE of the training and prediction sets [30, 31].The ANN was trained using a Powell-Beale restart training algorithm and calculating the derivatives with respect to the network parameters using the backpropagation algorithm. The ANN with 10 neurons per hidden per hidden layer was found to yield correct quantitative results with a minimum squared error (MSE) below 0.3.

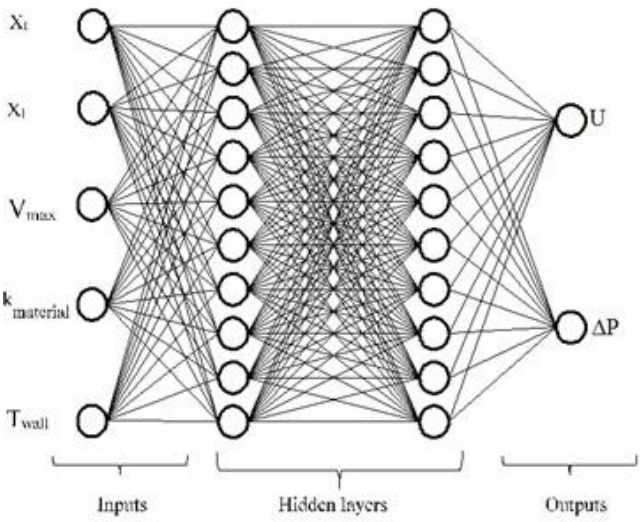

Figure 2. ANN architecture used. The X_t and X_l are the transverse and longitudinal distance, respectively. V_{max} is the maximum velocity, $K_{material}$ is the thermal conductivity of the material and T_{wall} is the wall temperature. These are the inputs variables and represent the system condition. U and Δ_p are the ANN prediction variables.

The ANN input layer are as follows: transverse X_t and longitudinal X_l distance, maximum velocity V_{max}, material thermal conductivity $K_{material}$, and wall temperature T_{wall}, while, pressure drop Δ_p and heat transfer global coefficient U were the output targets, as shown in Figure 2. All values were normalized between 0 and 1 for training and prediction of the ANN [32]. For the hidden layers, neurons were non-linear with tangent sigmoid transfer function (tanhsig) [33,34].

RESULTS AND DISCUSSIONS

Overall heat transfer coefficient and pressure drop were predicted through the assisted ANN model. The ANN exhibits good prediction capabilities as compared with the CFD simulated data for the four materials used. Pressure drop as well as overall heat transfer coefficient are in general well predicted, as can be seen in figures 3 to 5 and 6 to 8, respectively, for copper, aluminum and stainless steel, the ANN reproduces the general behavior of the data used for training.

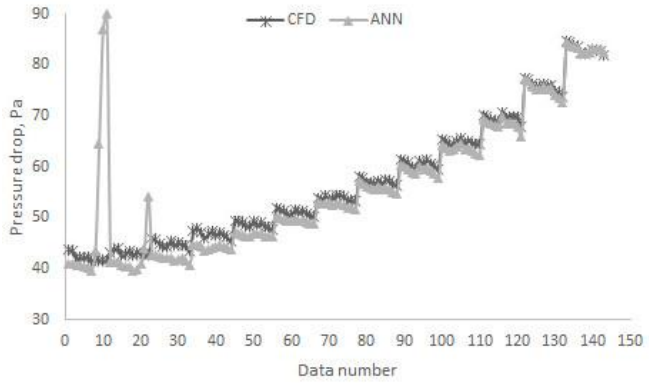

Figure 3. Results of pressure drop for copper pipes. Here, simulation (CFD) versus predicted (ANN) data are compared.

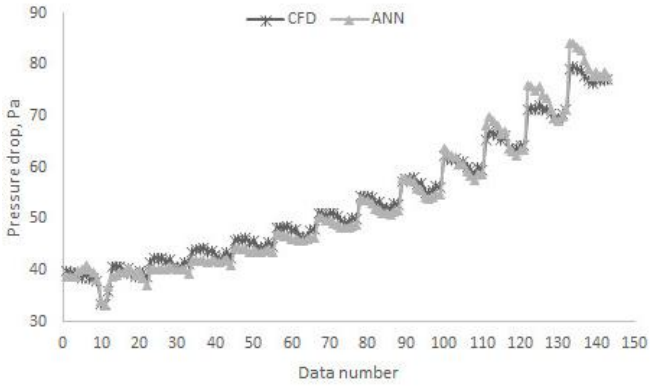

Figure 4. Results of pressure drop for stainless steel pipes. Here, simulation (CFD) versus predicted (ANN) data are compared.

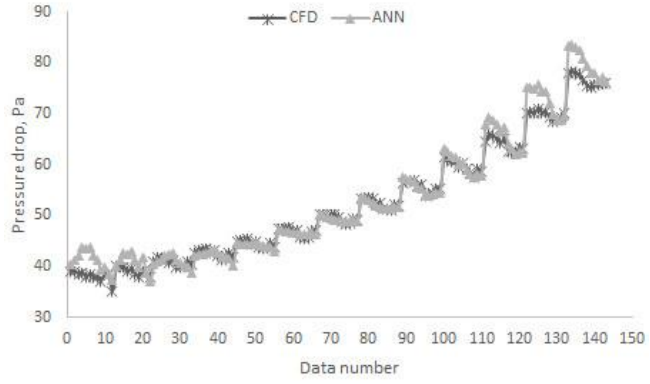

Figure 5. Results of pressure drop for titanium pipes. Here, simulation (CFD) versus predicted (ANN) data are compared.

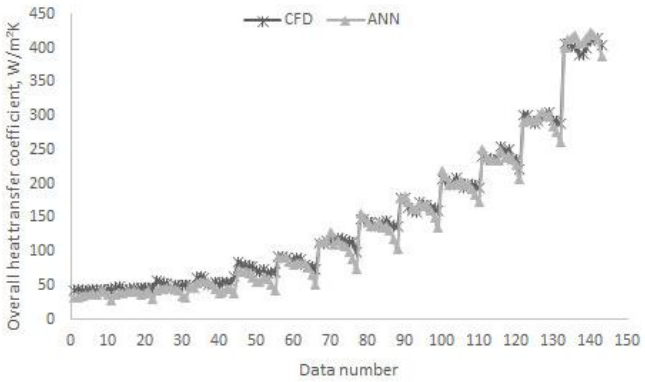

Figure. 6. Results of overall heat transfer coefficient for copper pipes. As before, simulation (CFD) versus predicted (ANN) data are compared.

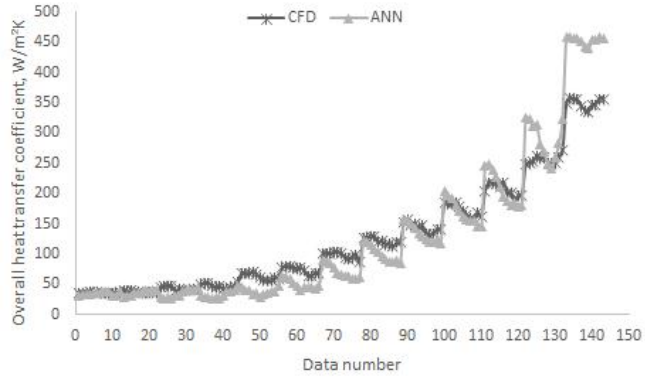

Figure 7. Results of overall heat transfer coefficient for stainless steel pipes. As before, simulation (CFD) versus predicted (ANN) data are compared.

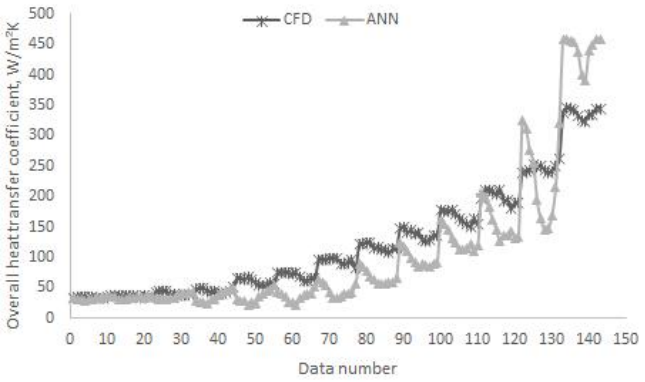

Figure. 8. Results of overall heat transfer coefficient for titanium pipes. As before, simulation (CFD) versus predicted (ANN) data are compared

The maximum deviation between predicted and simulated data for the overall heat transfer coefficients were calculated below of 0.4, 0.1 and 0.2% for copper, stainless steel, and titanium, respectively; while for pressure drop, the maximum deviations were below 0.1, 0.6 and 0.8% for the same materials (Figure 9 to 11).

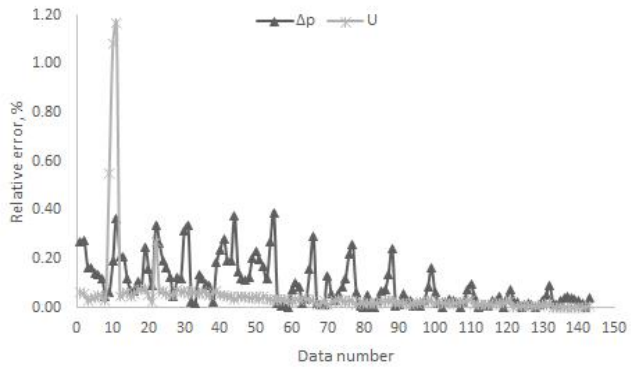

Figure. 9. Relative error for copper pipes data. Here, the pressure drop (Δ_p) relative error is below 0.1 %, while overall heat transfer coefficient (U) relative error is below 0.4 %.

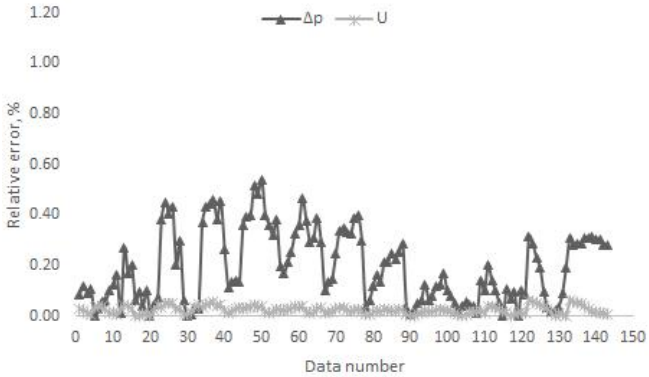

Figure. 10. Relative error for stainless steel pipes. Here, the pressure drop (Δ_p) relative error is below 0.6 %, while overall heat transfer coefficient (U) relative error is below 0.1 %.

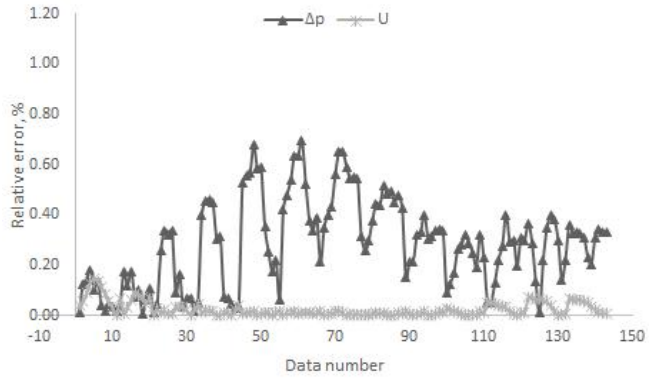

Figure. 11. Relative error for titanium pipes. Here, the pressure drop (Δp) relative error is below 0.8 %, while overall heat transfer coefficient (U) relative error is below 0.2 %.

In order to validate the generalization capabilities of the ANN we used a four material, aluminum, as test material. Once again heat exchanger simulation data were compared against the ANN prediction of the overall heat transfer coefficient and pressure drop. The results show that the ANN is capable of reproducing these variables although data for aluminum as heat exchanger material was not used for training, Figures 12 and 13. The maximum deviation between predicted and simulated data was found below 0.3 and 0.9% for overall heat transfer coefficient and pressure drop, respectively, as show Figure 14. These deviations compared favorably with those for the materials used for the training data.

Thus, the ANN constructed can predict the overall heat transfer coefficient and pressure drop independently of the material used, including the geometric arrange of the heat exchanger. This surrogate model can now be used for preliminary design purposes and optimization. For example, seeking a design that gives maximum heat transfer capability keeping a low pressure drop the models predicts a geometry with transversal and longitudinal section sizes of X_t = 0.022 and X_l = 0.063m, respectively, Δ_p = 69.87 Pa and U = 238.37 W/m^{2}K for copper, which is the best achievable compromise for the materials studied here. CFD simulation was used to verify these predictions, obtaining a pressure drop and overall heat transfer coefficient of Δ_p = 63.23 Pa and U = 226.90 W/m^{2}K, deviation well within the error acceptable for the design stage of the heat exchanger.

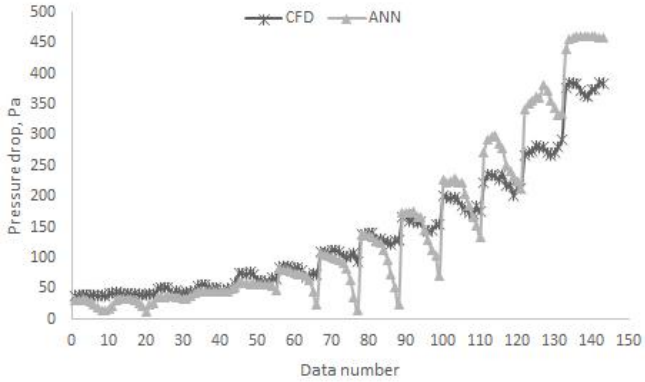

Figure. 12. Results of pressure drop for aluminum pipes. Data for aluminum were not included for training, the generalization capabilities of the ANN are validated in this manner.

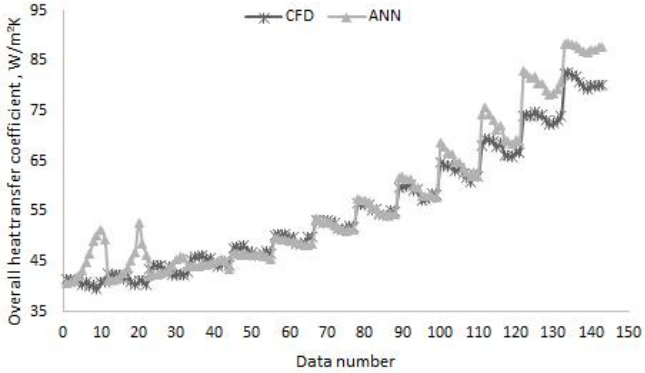

Figure. 13. Results of overall heat transfer coefficient for aluminum pipes. Data for aluminum were not included for training, the generalization capabilities of the ANN are validated in this manner.

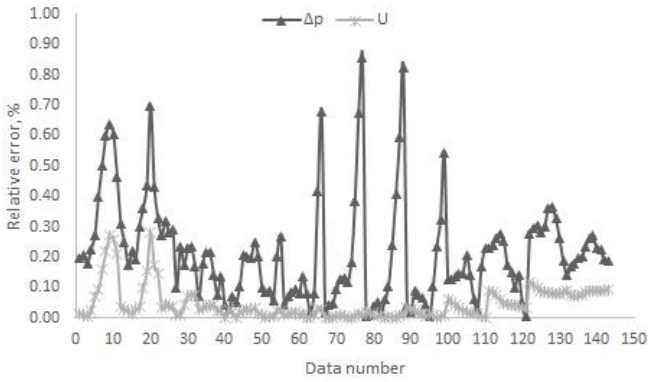

Figure. 14. Relative error of aluminum material. Here, pressure drop (Δ_p) relative error is below 0.9 %, while overall heat transfer coefficient (U) relative error is below 0.3 %.

Furthermore, the availability of the model can be the basis to assess the cost compromise between efficiency of the heat exchanger and its expected life cycle due to corrosion fouling requiring its replacement. Although the copper heat exchanger exhibits the maximum heat exchanger capacity, it has a smaller life cycle due to corrosion, and stainless steel may be preferred to build the heat exchanger. Stainless steel is constantly protected for a passive layer of Chrome oxide that naturally is generated in the surface when in contact with moist air. When the surface is damaged, the passive layer is regenerated making stainless steel a more resistant material for corrosive environments.

As summary, one can concluded that the ANN approach exhibits remarkable capabilities to generalize the complex dependence among variables, as shown in this case [35], simplifying the design and empowering its reach.

CONCLUSIONS

The aim of this work was to develop a predictive framework for the overall heat transfer coefficient and pressure drop for heat exchangers. Such framework is intended to facilitate the design and optimization of the exchanger configuration and material selection, allowing the inclusion of life-cycle data due to corrosion.

Here, the strategy was successfully tested with simulated data for four materials with 143 geometries for a crossflow heat exchanger that was numerically simulated through Computational Fluid Dynamics.

The robust predictive ANN model constructed lumps the behavior independently of the material used to simulate the heat exchanger, thus achieving a "general" predictor that can be applied to thermal analysis in engineering applications.

▪ ACKNOWLEDGMENTS

We acknowledge the Mexican Council of Science and Technology (CONACYT) for the scholarship granted for the development of this project.

REFERENCES

[1] Kakaç , S., Liu, H., Pramuanjaroenkij, A., 2012, Heat exchanger, selection, rating and thermal design, CRC PRESS, Taylor & Francis Group, Boca Raton, EUA, Chap. 1.

[2] Zukauskas, A.A., 1978, "Advances in Heat transfer", Academic Press, New York.

[3] Zukauskas, A.A., Ulinskas, R.V., 1978," Heat transfer efficiency of tube banks in crossflow at critical reynolds numbers," Heat Transfer-Soviet Research,10, pp. 9-15.

[4] Beale, S.B., Spalding, D.B., 1999, "A numerical study of unsteady fluid flow in in-line and staggered tube banks", Transactions of the CSME 1, 13, pp. 723-754.

[5] Kang, H.C., Kim, M.H.,1998," Effect of strip location on the airside pressure drop and heat transfer in strip fin-and-tube heat exchanger", International Journal of Refrigeration, 22, pp. 302–312.

[6] Yun, J.Y., Lee, K.S., 2000, "Influence of design parameters on the heat transfer and flow friction characteristics of the heat exchanger with slit fins", International Journal of Heat and Mass Transfer, 43, pp. 2529–2539.

[7] Qu, Z.G., Tao, W.Q., He, Y.L., 2004,"3D numerical simulation on laminar heat transfer and fluid flow characteristics of strip fin surface with X-arrangement of strip", Journal Heat Transfer, 126, pp. 69–707.

[8] Khan, W.A., Culham, J.R., Yovanovich, M.M., 2006," Convection heat transfer from tube banks in crossflow: analytical approach", International Journal Heat Mass Transfer, 49, pp. 4831–4838.

[9] Lee, C.K., Abdel-Monetm, S.A., 2001, "Computational analysis of heat transfer in turbulent flow past a horizontal surface with two-dimensional ribs", International Communications Heat Mass Transfer, 28, pp.161–170.

[10] Sahin, H.M, Dal, A.R, Baysal, E., 2007,"3D Numerical study on the correlation between variable inclined fin angles and thermal behavior in plate fin-tube heat exchanger", Applied Thermal Engineering 27, pp.1806-1816.

[11] Lam, K., Gong, W.Q., So, R.M., 2008, "Numerical simulation of cross-flow around four cylinders in an in-line square configuration", Journal of Fuids and Structures, 24, pp.34-57.

[12] Taher, F.N., Movassag, S.Z., Razmi, K., 2012, "Baffle space impact on the performance of helical baffle shell and tube heat exchangers", Applied Thermal Engineering,44, 143–149.

[13] Kim, T., 2013," Effect of longitudinal pitch on convective heat transfer in crossflow over in-line tube banks," Annals of Nuclear Energy; 57, pp.209–215.

[14] Sayed, A.E, Emad., Z.I, Osama, M.M., 2013,"Mohamed, A.A. Study of cross flow air-cooling

process via water-cooled wing-shaped tubes in staggered arrangement at different angles of attack, Part 2: Heat transfer characteristics and thermal performance criteria", International Journal Aerospace and Mechanical Engineering ,6,pp.1275-1288.

[15] Gharbi N.E., Kheiri, A., Ganaoui, M.E., Blanchard, R.,2015, "Numerical optimization of heat exchangers with circular and non-circular shapes", Case Studies in Thermal Engineering ,; 6: 194-203.

[16] Wang, Y. , Gu, X., Jin, Z., Wang, K. 2016,"Characteristics of heat transfer for tube banks in crossflow and its relation with that in shell-and-tube heat exchangers", International Journal of Heat Mass Transfer ,93,pp.584-594.

[17] Ishiyama, E. M., Paterson, WR, Wilson, D.I., 2011," Optimum cleaning cycles for heat transfer equipment undergoing fouling and ageing", Chemical Engineering Science,66, pp.604-612.

[18] Hu, S.M., Wang, S.H., Yang, Z.G., 2015," Failure analysis on unexpected wall thinning of heat-exchange tubes in ammonia evaporators", Case Studies in Engineering Failure Analysis ,3, pp. 52-61.

[19] Qian, Z., Seepersad, C.C., Joseph, V. R., Allen, J.K., Wu, C. J., 2006," Building surrogate models based on detailed and approximate simulations", Journal Mechanical Design", 128, pp. 668-677.

[20] Diaz, G., Sen, M., Yang, K.T., McClain, R.T., 1999," Simulation of heat exchanger performance by artificial neural networks", International Journal of HVAC&R Research,5, pp.195–208.

[21] Islamoglu, Y., Kurt, A., Parmaksizoglu, C., 2005," Performance prediction for nonadiabatic capillary tube suction line heat exchanger: an artificial neural network approach", Energy Conversion Management, 46, pp.223–232.

[22] Xie, G.N., Wang, Q.W., Zeng, M., Luo, LQ., 2007, "Heat transfer analysis for shell-and tube heat exchangers with experimental data by artificial neural networks approach", Applied Thermal Engineering,27, pp.1096–1104.

[23] Xie, G.N., Sunden, B., Wang, Q., Tang, L., 2009, "Performance predictions of laminar and turbulent heat transfer and fluid flow of heat exchangers having large tube-diameter and large tube-row by artificial neural networks", International Journal of Heat and Mass Transfer ,52,pp. 284–2497.

[24] Yakhot, V., Smith, L.M., 1992, "The renormalization group, the ε-expansion and derivation of turbulence models", Journal of Scientific Computing, 7, pp.35–61.

[25] Launder B.E., Spalding, D.B., 1974, "The numerical computation of turbulent flows", Comput Methods Appl Mech Eng,3,pp.269-289.

[26] Pérez-Segarra, C, Oliva, A, Costa, M., Escanes F., 1995, "Numerical experiments in turbulent natural and mixed convection in internal flows", International Journal of Numerical Methods for Heat & Fluid Flow, 5, pp.13-33.

[27] Patankar, S.V., 1980, "Numerical heat transfer and fluid flow", Taylor and Francis, London.

[28] Roache, P.J. 1998, "Fundamentals of computational fluid dynamics", Hermosa Publisher, Albuquerque, Nuevo México.

[29]. Tlatelpa-Becerro, A, Rico-Martínez, R. Castro-Gómez, L., Urquiza, G., Calderón-Ramirez, M., 2018, "Artificial Neural Networks (ANN) and Kalman Filter Algorithms to Predict Output Temperatures on a Heat Exchanger", International Journal of Applied Engineering Research, 13, pp. 13130-13135.

[30] Khataee, A.R., Kasiri, M.B., 2005, "Artificial neural networks modeling of contaminated water treatment processes by homogeneous and heterogeneous nanocatalysis", Journal of Molecular Catalysis A: Chemical ,331, pp.86-100.

[31] Simon, H., 1999, Neural networks and learning machines, Person, NY.

[32] Sencan, A., Kalogirou, S.A., 2010, "A new approach using artificial neural networks for determination of the thermodynamic properties of fluid couples", Energy Conversion and Management ,46, pp. 2405–2418.

[33] Hikmet E., Mustafa I., 2009," Modelling of a vertical ground coupled heat pump system by using artificial neural networks", Expert Systems with Applications ,36, pp.10229–10238.

[34] Sencan, A., Kemal, A.Y., Soteris, A.K., 2006, "Thermodynamic analysis of absorption systems using artificial neural network", Renewable Energy,31, pp. 29–43.

[35] Humphrey, G.B., Maier, H.R., Wu, W., Mount, N.J., Dandy, G.C., Abrahart, RJ, Dawson, C.W., 2017, "Improved validation framework and R-package for artificial neural network models", Environmental Modelling & Software,92, pp. 82-106.